Int. J. Electrochem. Sci., 12 **(2017)** 10152 – 10176, doi: 10.20964/2017.11.86

International Journal of
ELECTROCHEMICAL
SCIENCE
www.electrochemsci.org

Failure Pressure Estimations for Pipes with Combined Corrosion Defects on the External Surface: A Comparative Study

G. Terán[1], S. Capula-Colindres[1], J.C. Velázquez[1,2*], M. J. Fernández-Cueto[3], D. Angeles-Herrera[4], Héctor Herrera-Hernández[5]*

[1] Departamento de Ingeniería Química Industrial, ESIQIE, IPN, UPALM EDIF. 7, Zacatenco, Mexico City, Mexico CP 07738.
[2] Gerencia de Ingeniería y Costos, Pemex Transformación Industrial, Petróleos Mexicanos, Piso 6, Edificio B1, Marina Nacional 239 Col. Petróleos Mexicanos, Mexico City, Mexico, CP 11311.
[3] Instituto Tecnológico de Tuxtepec, Av. Dr. Victor Bravo Ahuja s/n, col. 5 de Mayo Tuxtepec, Oaxaca, Mexico, CP 68350.
[4] Instituto Mexicano del Petróleo, Eje central Lázaro Cárdenas 152, Col. San Bartolo Atepehuacan, Mexico City, Mexico, CP 07730.
[5] Universidad Autónoma del Estado de México, IIN-Lab. de Electroquímica y Corrosión de Materiales Industriales, Blvd. Universitario s/n, Predio San Javier Atizapán de Zaragoza, Estado de Mexico 54500, Mexico.
[*]E-mail: gerardoteranm@gmail.com, jcva8008@yahoo.com.mx

Received: 10 July 2017 / *Accepted:* 21 September 2017 / *Published:* 12 October 2017

In this research paper, the failure pressure predictions were obtained for a pipeline section by analyzing a combined corrosion defects, which joins together a general corrosion and a pitting corrosion defects. Well-known conventional mathematical methods were used in this study to predict the failure pressure of corroded steel pipelines, such as: B31G, RSTRENG-1, Shell-92, DNV, PCORR, and Fitnet FFS. The equations reported for corrosion defects with more complex characteristics developed by Choi *et al.,* and Cronin *et al.* were also used. Furthermore, Finite Element (FEM) is one of the most employed nonlinear methods because of its good response of pipeline failure prediction under the corrosion mechanism. So, FEM methodology results the least conservative in comparison with the others mathematical models, according to the literature, for this reason it was used to compare the standard deviation σ of the methods. Failure pressure predictions determined that the most conservative methods were: Shell-92, Fitnet FFS, Choi's method, B31G, RSTRENG-1, Cronin´s method, PCORR and DNV, in that order.

Keywords: Corrosion Defect, Pipeline Steels, Failure Pressure and Finite Element Method.

Nomenclature	
A%	relative elongation
C_D	corrosion depth
C_o, C_1, C_2	Choi´s method constants
D	external pipeline diameter
E	modulus of elasticity
g	geometry factor
K	hardening coefficient
L	longitudinal corrosion defect length
M	bulging factor
P_D	pit depth
pf	failure pressure
$p_{LongGroove}$	failure pressure of long groove
$p_{PlainPipe}$	failure pressure of plain pipe
p_{2Inst}	instability pressure of plain pipe
RE	relative error
r	current inside pipe radius
t	pipe wall thickness
t_{Lo}	original ligament thickness
y	defect depth
ν	Poisson´s ratio
σ_{YS}	material yield stress
σ_{UTS}	material ultimate tensile stress
σ_{crit}	critical stress at failure
t_{LO}	original ligament thickness at the deepest point in the defect
ε_{cri}	critical strain
α and n	Ramberg-Osgood material parameters
σ_1	axial stress acting along the longitudinal direction
σ_2	hoop stress acting along the circumferential/tangential direction
σ_3	radial stress acting along the radial direction
σ_{VM}	Von Misses stress

1. INTRODUCTION

According to the last study presented by NACE in 2016 titled “International Measures of Prevention, Application, and Economics of Corrosion Technologies Study” [1] the global cost of corrosion is equivalent to 3.4% of the GDP (Gross Domestic Product) and it demonstrated that by using available corrosion control methods, it is feasible to save up to 35% of the corrosion cost. In this study, NACE emphasizes that the oil and gas industry is one of the sectors that invest the most in corrosion control and monitoring. In this industry, buried pipelines constitute a safe, efficient and low-cost means of hydrocarbon transportation that satisfies the demand for petroleum in different parts of the world. Oil and gas pipelines are being used in different environmental conditions, such as arctic, desert, jungle, tropical forests, and so on. In Mexico, the external damage in oil and gas pipelines is mainly motivated by the localized corrosion defects [2]. In this sense, it is worthwhile to study the influence of corrosion on the lack of pipeline hermeticity and how it causes a great number of small

leaks. For this reason, it is important to model the time evolution of the external localized corrosion defects [3,4] in order to evaluate pipeline reliability [5].

The analytical methods for estimating the pipeline failure pressure are based on the corrosion defect depth and length. The traditional methods for estimating the failure pressure in a corroded pipeline are: B31G [6], RSTRENG-1 [7], PCORR (Batelle) [8], DNV-99 [9], Shell [10], Fitnet FFS [11]. However, one feature of B31G and RSTRENG-1 methods is that the pressure failure values can be more conservative[1] than the others [12-18]. However, there are other options for estimating the failure pressures in pipelines with different corrosion defect profiles. Filho *et al*. [12], presented equations with a single pit in an API-5L-X65 pipelines. This study is limited to a single pit and it did not consider another type of corrosion. Bin Ma *et al*. [19] proposed equations in different pipeline steels using corrosion profiles, such as elliptical-shape defects with high stress yields. This equation is not applied to steels with low stress yield, such as steel API 5L X42 or API 5L X56. Another shortcoming of these studies could be that the failure pressure is only useful for a single pit. Lee *et al*. [20] proposed equations for two rectangular pitting in longitudinal and circumferential directions. They do not, consider the interaction of any other types of corrosion, such as general corrosion. Cronin *et al*. [15] presented a method based on complex corrosion defects using the weighted depth difference (WDD). Less conservative values between 20 and 34% are achieved in comparison to B31G and RSTRENG, respectively. Choi *et al*. [14] proposed equations for an API 5L X65 pipeline with a rectangular-shaped defect, getting adequate results when comparing their values to experimental failure pressures. The Finite Element Method (FEM) has been conducted frequently to get failure pressure predictions in pipelines with complex corrosion defects. Machado *et al*. [21] confirmed that FEM predictions produced more accurate results when these were compared with other methods. Using FEM allows for the evaluation of corrosion defects with complex geometries, getting better results than traditional methods [12].

According to the literature, there are several studies of corrosion defects using FEM with different geometries, such as oval-shaped defects [22], elliptical-shaped defects [17,19,23,24], ellipsoid-shaped defects [25], holes-shaped defects [12], groove-shaped defects [14,26], long blunt grooves [23,24,26,27], rectangular-shaped defects [14], semi-spherical shaped defects [23,24], and pitting [20,28,29]. So far, there are only a few studies where two types of corrosion defects are analyzed together in pipe segments. Recently, Bedairi *et al*. [16] has presented a new hybrid defect in pipelines, which occurs in cracks in corrosion (CIC). The CIC model combines a corrosion defect with a flat bottom and in this a crack of uniform depth. This combination is based on the fact that it is possible to find two corrosion defects in pipelines.

Therefore, in the present study, the aforementioned traditional methods (B31G, RSTRENG-1, PCORR, DNV-99, Shell, Fitnet FFS), Cronin and Choi were used to obtain the failure pressure predictions for a combination of two types of external corrosion defects (general corrosion in a rectangular-shaped defect with spherical ends and a spherical-shaped pitting) on a pipe surface. One limitation of the traditional methods is that they depend on perfect corrosion profiles in order to predict the failure pressure values in pipelines with general or localized corrosion and they do not consider the

[1] In this paper, the word "conservative" refers to lower numerical values of failure pressure estimated by methods in comparison with the failure pressure estimation using FEM.

stress concentration motivated by complex geometries in pitting corrosion. In this context, it is necessary to include another technique, such as FEM, in order to obtain the failure pressure predictions in pipelines. The aim of this study is to compare the failure pressure predictions achieved with both traditional methods and FEM. The combined corrosion defect is studied in an API 5L X52 steel pipe section. In addition, the mechanical behavior of the pit was also analyzed by FEM, through Von Mises stress against internal pressure plots.

2. SOIL CORROSIVITY AND ITS ELECTROCHEMICAL BEHAVIOR

In Mexico, almost the majority of the leaks occur by pits that grown-up on the external surface of the buried steel pipes [2]. Some studies have indicated that the soils in the south side of Mexico (Veracruz, Tabasco and Chiapas) are a kind of silty clay [3-4, 49-50]. These soils are slightly acidic (pH 6.13) with a chloride content of about 47 ppm and the pipelines that work in that zone are, in general terms, cathodically protected (pipe-to-soil potential about −880 mV) [3-4, 49-50]. From all the soil characteristics analyzed in the aforementioned research, the variables that exert the greatest influence are pH, pipe-to-soil potential (E_{corr}), soil texture, water content and dissolved chloride concentration, in that order. Similar results were found by Kar Sing Lim et al. in a paper published in 2017 for Malaysian soils [53].

While analyzing the electrochemical behavior of a pipeline steel immersed in a simulated soil solution, it was found that the corrosion potential (E_{corr}) has a minimum value after 168 h of immersion [54]. It means that after this time the formation of corrosion products is more efficient and they can provide a better protection on the steel surface. This conclusion also agrees when the Linear Sweep Characterization is done for pipeline steel. In this experimental technique, it is possible to observe that in the first 24 hours the steel surface is almost free of corrosion products [54]. According to the X-ray diffraction characterization, the main corrosion products found in a solution that simulates the chemical composition of Mexican soil are magnetite (Fe_3O_4), maghemite (γ-Fe_2O_3), goethite (α-FeOOH) and lepidocrocite (γ -FeOOH) [54]. The composition of these compounds is dependent on exposure time.

After analyzing the soil corrosivity, its electrochemical behavior, and the frequency with which external corrosion defects appear, it is important to study the impact of the geometry of the corrosion defects and the methods used to assess the pipeline integrity under working pressure. One of the purposes of the study is to complement the knowledge of the soil corrosion with computational techniques to determine the pipeline's reliability.

3. EXPERIMENTAL PROCEDURE

3.1 Mechanical properties of a pipeline steel (API 5L X52)

API 5L X52 steel is one of the most common pipeline material used for oil and gas transmission. The chemical composition and mechanical properties of samples of this steel are shown

in Table 1 and Table 2, respectively [23,24]. In Fig. 1, the true stress-strain curve of an API 5L X52 steel with the hardening effect is illustrated.

Table 1. Chemical composition of API X52 pipeline (weight %) [**23, 24**].

C	Mn	Si	Cr	Ni	Mo	S	Cu	Ti	Nb	Al
0.22	1.22	0.24	0.16	0.14	0.06	0.036	0.19	0.04	<0.05	0.032

Table 2. Mechanical properties of API X52 pipeline [**23, 24**].

E (GPa)	ν	σ_Y (MPa)	σ_{UTS} (MPa)	A%	n	K (MPa)
203	0.30	410	528	32	0.164	876

E (GPa), ν, σ_Y, σ_U, A%, n and *K*, are modulus of elasticity, Poisson´s ratio, yield stress, ultimate stress, relative elongation, hardening exponent and hardening coefficient, respectively.

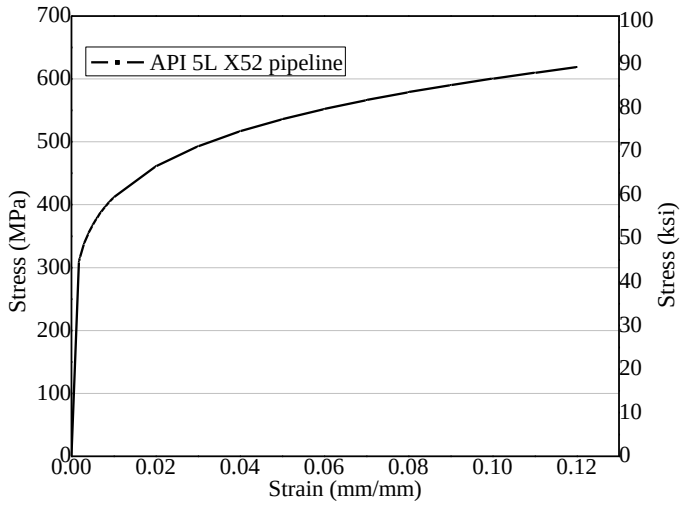

Figure 1. True stress-strain curve for API 5L X52 pipeline steel **[23,24].**

3.2 Failure pressure (P_f)

Table A1 in the appendix of this paper shows the equations commonly used to estimate the pipeline failure pressure. In this study, the maximum depth (50%) of pipeline wall thickness, which is the sum of the two corrosion defects, general corrosion (25%) and pitting corrosion (25%), is adopted to obtain the failure pressure values. To determine the failure pressure values by Cronin's method [15], the values for *g*, σ_{crit}, $\mathcal{E}_{crit}$, α and *n* were 0.756, 600 Mpa, 0.105, 5.87 and 8.24, respectively. One limitation in Cronin's study [15], regarding the parameter *g*, is that it depends on the weighted depth difference (WDD) method, and *g* can be obtained using specialized software, such as the CPS (corrosion profile shaded). For the current study, the parameter *g* is considered zero for all conditions.

3.3 FEM simulations

A set of nine conditions were modeled to estimate the failure pressure values, which use the corrosion defect length (L) and the wall thickness (t) as variables. In Fig. 2, the shape and size of the corrosion defect studied is illustrated, while Fig. 2a) shows the general view of the pipe section and Fig. 2b) presents an overview of the pipe section undergoing a combination of two types of simulated corrosion defects. The pipeline diameter (D) is 609.6 mm for all conditions. Fig. 3 shows the pit dimensions and its geometry. Table 4 summarizes all cases in the present study.

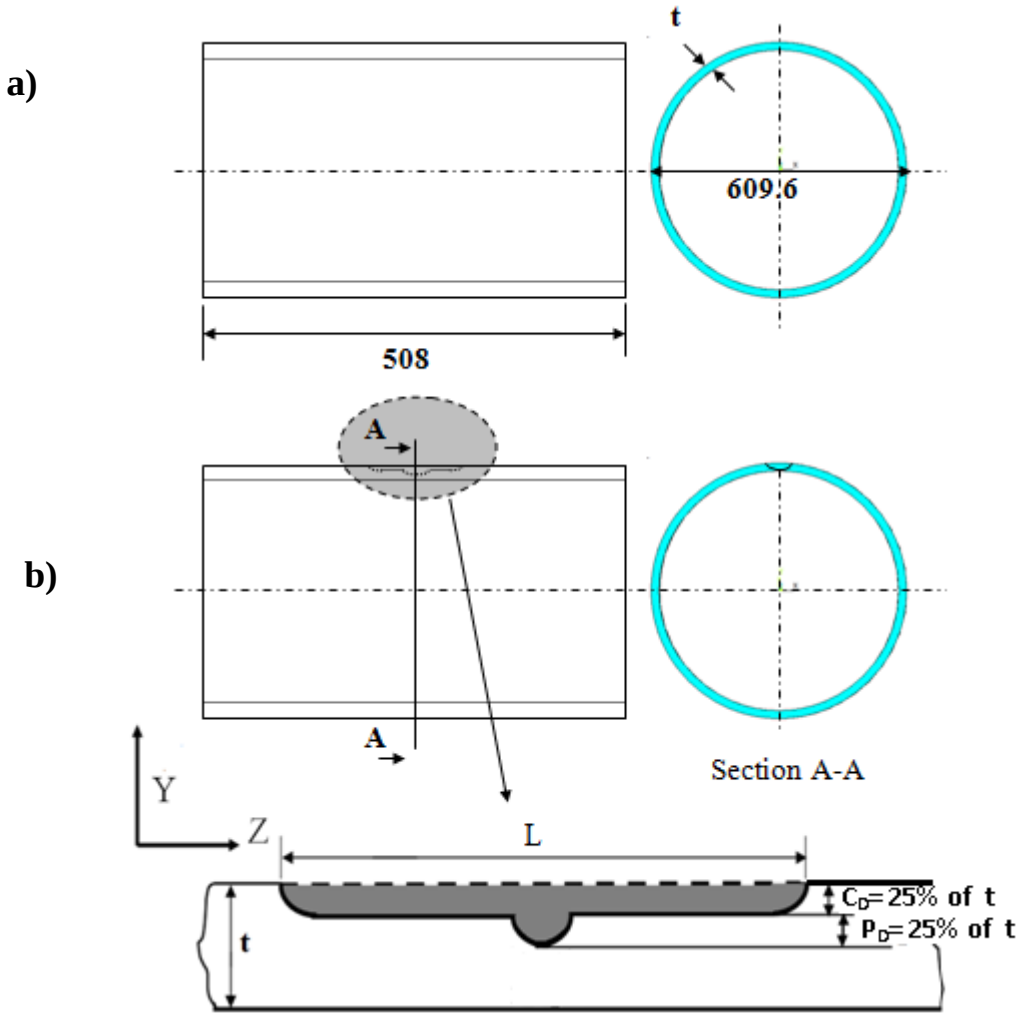

Figure 2. Pipeline geometry (all dimensions in millimeters): a) circumferential and longitudinal pipeline and b) corrosion defect. (C_D and P_D refers to general corrosion depth and pitting depth, respectively)

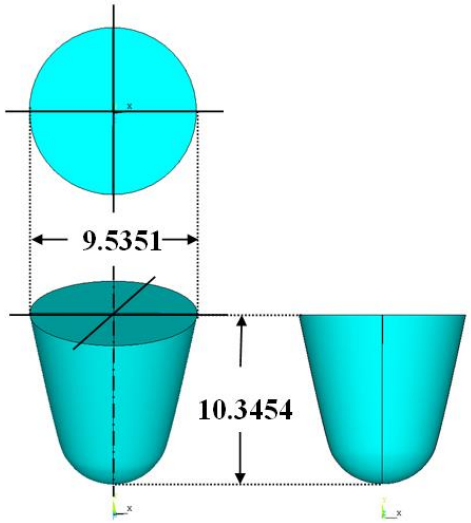

Figure 3. Semi-elliptical pit (dimensions in millimeters).

Table 4. Summary of FEM analysis.

	t thickness	L Length	C_D+ General Corrosion Defect Depth	P_D* Pitting Corrosion Defect depth
Case	mm	mm	mm	mm
1	9.525	152.4	2.387	4.775
2	9.525	304.8	2.387	4.775
3	9.525	609.6	2.387	4.775
4	12.7	152.4	3.175	6.35
5	12.7	304.8	3.175	6.35
6	12.7	609.6	3.175	6.35
7	19.05	152.4	4.775	9.525
8	19.05	304.8	4.775	9.525
9	19.05	609.6	4.775	9.525

+ 25% of pipe wall thickness

*25% of pipe wall thickness

To create 3D models with FEM, plain strain conditions were considered to restrict the pipeline from expanding or contracting longitudinally [16]. Due to the pipeline's symmetric geometry, one quarter of the pipe was considered as presented in Fig. 4a) and b).

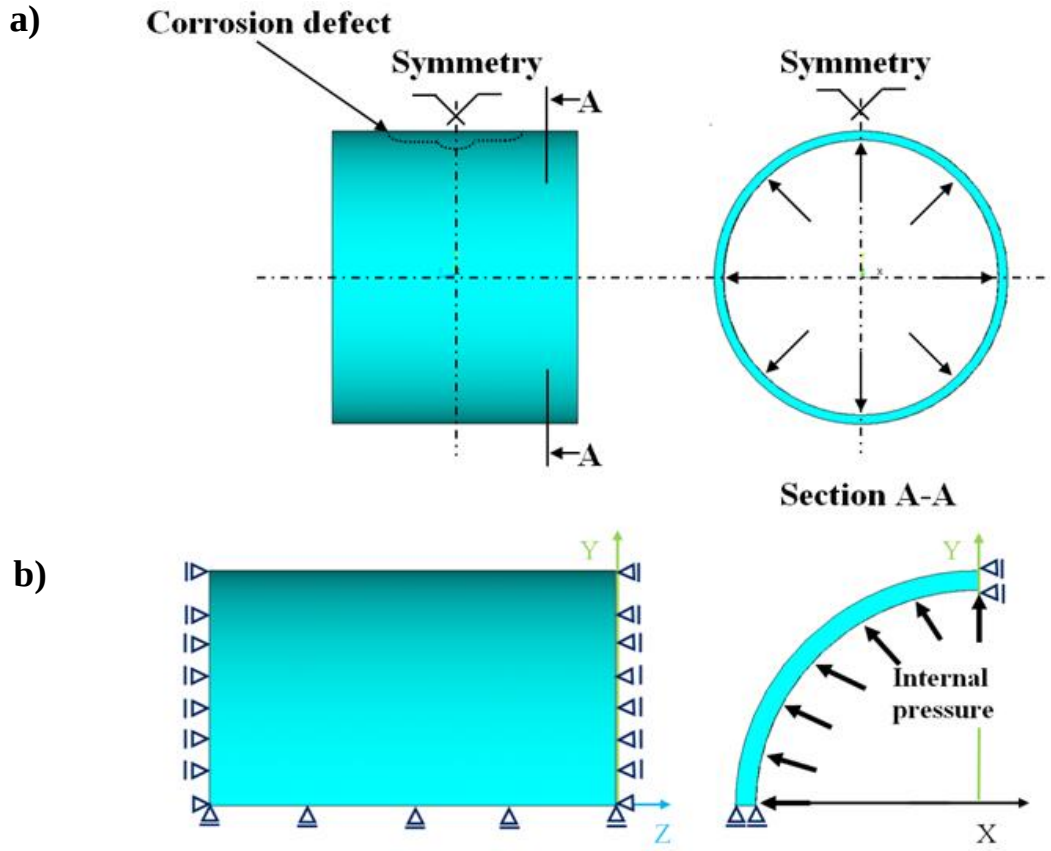

Figure 4. Symmetry conditions: a) symmetry in longitudinal and transverse direction and b) boundary conditions.

FEM has been widely used to investigate the failure pressure estimations with corrosion defects [15,30-33]. To mesh a 3D model, brick solid 45 isoparametric elements were employed. The total number of elements and nodes were approximately 2000 and 15000 respectively. The commercial software ANSYS version 11.2 was adopted [34]. Cronin *et al*. [15] employed 2 elements through the pipeline thickness to determine the failure pressure values. Bedairi *et al*. [16] used 10 elements in 3D pipeline models affected by corrosion. For the present study, 2 and 3 elements were selected to mesh the corrosion defect in a pipe section. Considering the symmetric condition, only one quarter[2] of the pipeline with the two corrosion defects was modeled, see Fig. 5a) and Fig. 5b) that presents the mesh used for all conditions. A material with elastic-plastic, isotropic, hardening behavior was adopted as well, as the Von Mises criterion was employed [12]. Both material nonlinearity and large displacement were conducted in the elastic-plastic analysis. In the study by FEM, the failure pressure values are considered when Von Mises stresses[3] reach maximum stresses of the material, whose stresses values are equal to the whole area of ligament[4] [12,16,19,35,36]. In the pipelines, Von Mises criterion is applied since the three principal stress components act along the axes of the pipeline [37]:

[2] For the sake of simplicity and because of the pipeline symmetry in Finite Element Analysis, it is common to model only one quarter of the specimen.
[3] Von Mises stress is widely used by engineers to verify whether the pipe or the vessel will withstand a given load condition.
[4] In this paper, the word "ligament" has the same meaning as "remaining pipe wall thickness".

$$\sigma_{VM} = \left(\frac{1}{\sqrt{2}}\right)\sqrt{(\sigma_1-\sigma_2)^2+(\sigma_2-\sigma_3)^2+(\sigma_3-\sigma_1)^2} \quad [1]$$

Where:

σ_1= axial stress acting along the longitudinal direction

σ_2= hoop stress acting along the circumferential/tangential direction

σ_3= radial stress acting along the radial direction

σ_{VM}= Von Misses stress.

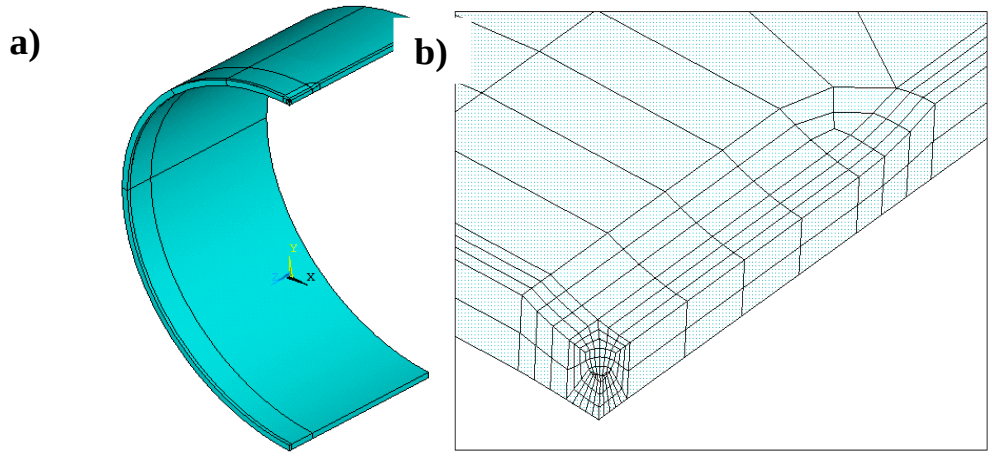

Figure 5. 3D model for an API 5L X52 pipeline: a) a quarter of the pipe and b) finite element mesh for two corrosion defects.

4. RESULTS AND DISCUSSION

4.1 Failure pressure (P_f) estimation

Table 5 presents the failure pressure values estimated by different methods and FEM. Table 6 gives the mean error (%) of each method against FEM, considering this as the most realistic model [12,24].

It is pointed out that for the methods and FEM the failure pressure values decrease as the corrosion defect depth and length increase with constant pipeline thickness. For all methods, the results were determined for a total corrosion depth of 50% of the pipe wall thickness; as a result, the failure pressure decreases. This is because the corrosion defect removed enough material of the pipe wall thickness, weakening the ligament and resulting in low failure pressure. The failure pressure values were obtained by Cronin's method considering a *g* parameter value of 0.756. The failure pressures decrease as the corrosion defect length increases when values of *g* that were less than 1 were obtained. However, it is assumed that these decreases could be small as the corrosion defect length increases. The *g* parameter was applied from the CPS Software, and it depends on the length and depth of the corrosion defect.

Table 6 showed the mean error as a percentage (%) among the traditional methods respecting FEM. Since all cases showed the same behavior, only cases 1, 4 and 7, where the wall thickness of the

pipeline (*t*) was changed, were considered. It is possible to observe that Shell-92 method was the most conservative, followed by Fitnet FFS, Choi's method, B31G, RSTRENG-1, Cronin's method, PCORRC and DNV. To obtain the mean error (%), the following equation was used:

$$\left[\frac{P_f\left(methods\right)-P_f\left(FEM\right)}{P_f\left(MEF\right)}\right]x100 \qquad [2]$$

Table 5. Comparison of failure pressure estimation values by methods and FEM results, in MPa.

*	B31G	RSTRENG-1	Shell-92	DNV	PCORRC	Fitnet FFS	Choi	Cronin	FEM
1	11.22	11.14	9.80	12.57	12.64	9.92	11.17	12.65	15.37
2	10.35	9.91	8.56	10.52	10.58	8.66	9.39	12.65	15.09
3	7.87	9.33	7.96	9.39	8.90	8.05	4.24	12.65	14.89
4	15.30	15.33	13.57	17.55	17.39	13.81	15.37	16.87	20.85
5	14.01	13.50	11.69	14.59	14.71	11.89	13.00	16.87	20.27
6	10.52	12.58	10.75	12.85	12.25	10.94	5.82	16.87	20.06
7	23.69	24.04	21.51	28.05	27.08	22.12	23.92	25.31	32.92
8	21.47	20.90	18.18	23.27	23.29	18.70	20.57	25.31	31.19
9	15.79	19.15	16.44	20.07	19.29	16.90	9.00	25.31	30.75

*cases

Table 6. Mean error (%) by methods

*	B31G	RSTRENG-1	Shell-92	DNV	PCORRC	Fitnet FFS	Choi's method	Cronin's method
1	27	28	36	18	18	35	27	18
2	31	34	43	30	30	43	38	16
3	47	37	47	37	40	46	72	15
4	27	26	35	16	17	34	26	19
5	31	33	42	28	27	41	36	17
6	48	37	46	36	39	45	71	16
7	28	27	35	15	18	33	27	23
8	31	33	42	25	25	40	34	19
9	49	38	47	35	37	45	71	18

*condition

4.2 Effect of corrosion defect length

Figure 6 shows the failure pressures against corrosion defect lengths for all methods and FEM. In this figure, the failure pressure values are illustrated for different corrosion defect lengths: a) 9.525 mm, b) 12.7 mm and c) 19.05 mm. In general, the failure pressure values determined by the well-established methods show lower values compared to FEM. The most conservative methods are: Shell-

92, Fitnet FFS, B31G, RSTRENG-1, Choi's method, Cronin's method, PCORR and DNV, in that order.

Figs. 6a), b), and c) show the failure pressures for different corrosion defect lengths as a function of the wall thickness (*t*) of 9.525 mm, 12.7 mm and 19.05 mm, respectively. The wall thickness of 9.525 mm is used for cases 1 to 3, 12.7 mm for cases 4 to 6 and finally 19.05 mm for cases 7 to 9. It is also demonstrated that there is a significant dependence of failure pressures in the corrosion defect length for the analytical methods. In this sense, as seen in Fig. 6a), it is possible to observe that all failure pressure estimations are close numerically for 9.525 mm corrosion defect length. On the other hand, in Fig. 6b) and c), one can see that the failure pressure estimations for 12.7 mm and 19.05 mm corrosion defect lengths are more dispersed. However, when the corrosion defect length is greater (L≥300-600 mm), the failure pressures decreases. The results obtained by traditional methods are less accurate when the corrosion defect length is larger and they should not be used to analyze the larger corrosion defects.

a)

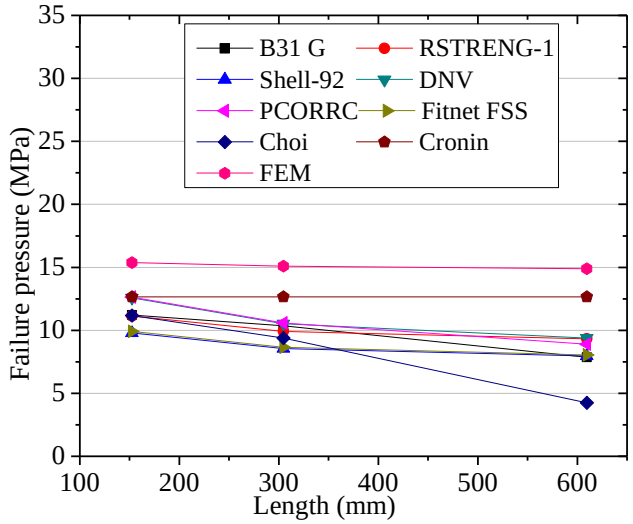

b)

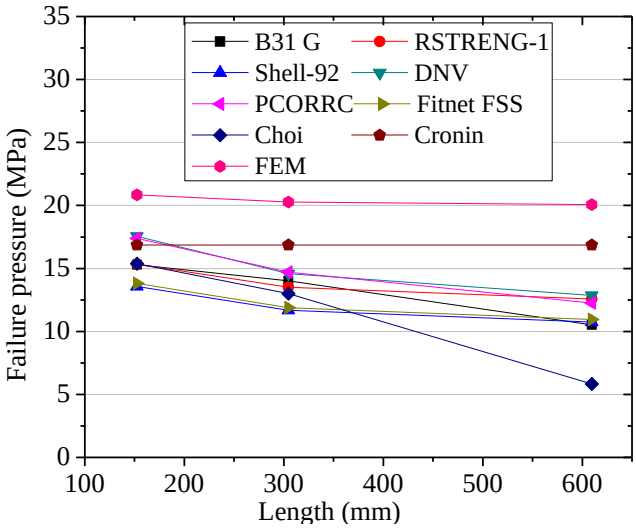

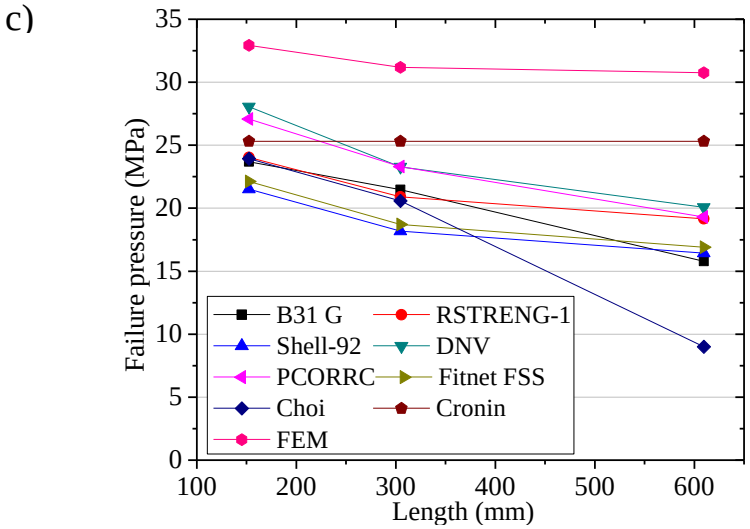

Figure 6. Failure pressure values of pipelines as a function of the corrosion defect length for several pipeline wall thicknesses, a) 9.525 mm, b) 12.7 mm and c) 19.05 mm.

This is because the background of these methods is established on short corrosion defects. Finally, FEM (whose failure pressure values were highest out of all corrosion defect lengths) revealed minimal differences of failure pressures with respect to all corrosion defect lengths. It means that FEM is less sensitive to corrosion defect lengths.

4.3. Effect of corrosion defect depth

Figs. 6a), b), and c) show the failure pressures for corrosion defect depth as a function of wall thickness (t) of 9.525 mm, 12.7 mm and 19.05 mm, respectively. This is because the wall thickness of 9.525 mm pertains to cases 1-3, 12.7 mm to cases 4 to 6 and 19.05 mm to cases 7 to 9.

Fig. 7 shows the failure pressure based on the variation of the corrosion defect depth: a) 4.775 mm, b) 6.35 mm and c) 9.525 mm. It is noted that the failure pressures increase as corrosion defect depth increases. Both the defect caused by general corrosion and the defect caused by pitting corrosion have, in total, a depth of 50% of the wall thickness (t), which is considerably deep. The total depth of the two corrosion defects is the sum of 25% of the wall thickness for general corrosion defect depth and 25% of the wall thickness for pitting depth. These figures also show a similar behavior described in Section 3.2, where it was observed that failure pressure estimations were closer in numerical value for all the traditional methods (Fig. 7a), and when the corrosion defect depth increases, the results were more dispersed (Fig. 7b) and c).

Analyzing the results, the most conservative estimations are achieved by Shell-92, Fitnet FFS, B31G, RSTRENG-1, Choi's method, Cronin's method, PCORR and DNV, in that order. FEM always has the highest failure pressure values.

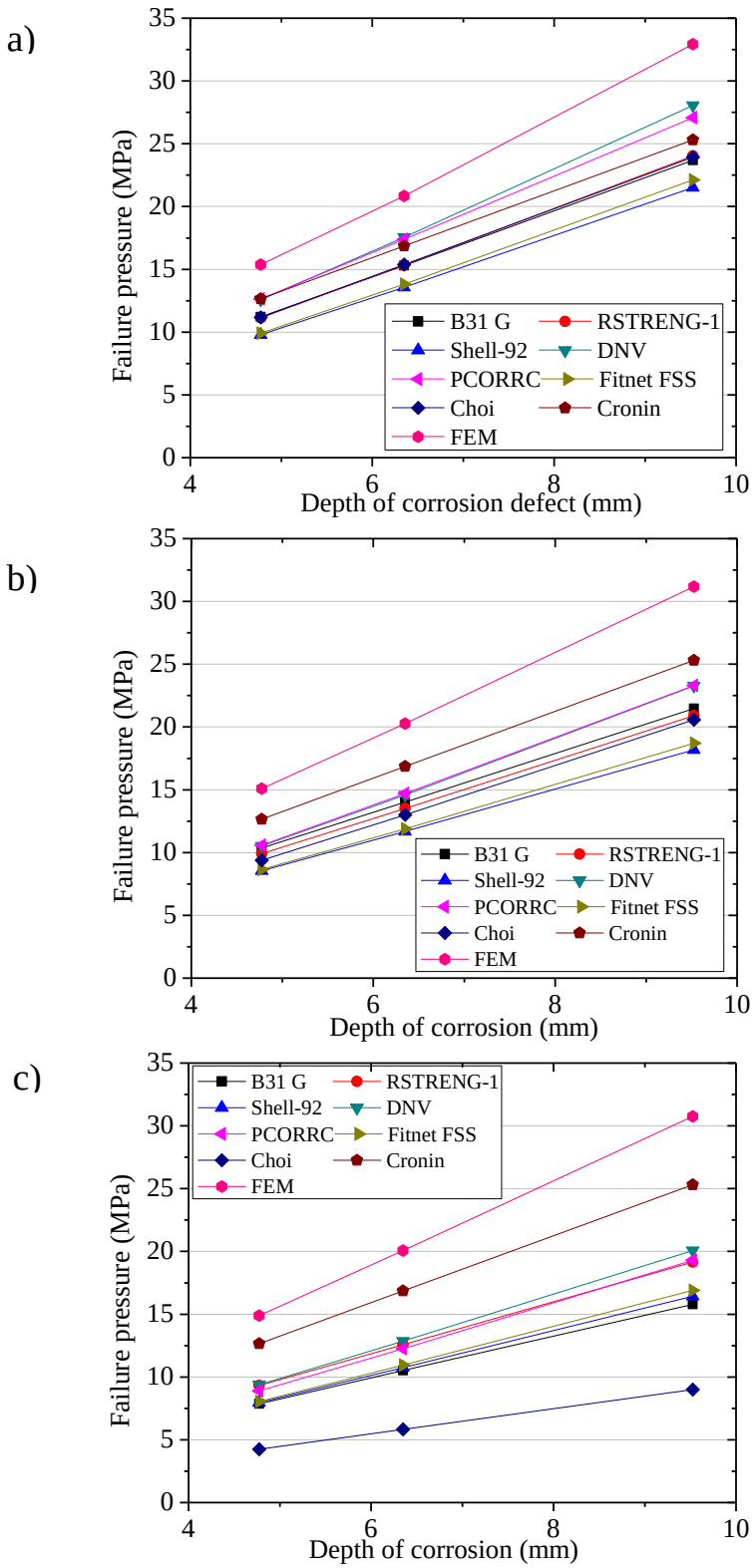

Figure 7. Failure pressure values of pipelines as a function of the corrosion defect depth, a) 9.525 mm, b) 12.7 mm and c) 19.05 mm.

For all methods used in this research, the failure pressures data was lower than FEM. All results were less than 1 when the relative error (RE) was employed. That is, the failure pressure was underestimated. The RE can be obtained using the following equation [17].

$$RE = \frac{Failure\ pressure\,(methods)}{Failure\ pressure\ (FEM\ \mathrm{mod}\,el)} \quad [3]$$

As the RE values were less than 1, the pipeline with a combined corrosion defect can be operated relatively safely under moderated pressure conditions. A rupture analysis is recommended to reveal the effect of bulging factor[5], particularly where stress is highest at the defect area [37]. Although such high levels of conservatism ensure additional safety, it can also lead to cost elevation due to unnecessary repairs and replacement of in-service pipeline sections [26].

Shell, Fitnet FFS and B31G methods obtained conservatives values of failure pressures respecting FEM. This is due to the three methods adopting the same bulging factor (M), which is conservative. Therefore, enough material is removed, resulting in a high stress in the ligament; as a consequence, low conservative failure pressure values were produced. Fitnet FFS method based its approximation of failure pressure on an ideal corrosion defect where enough material is removed. The mean errors (%) were 35-45% and 36-47% for the Fitnet and Shell methods, respectively, when compared against FEM.

B31G method shows two equations for pressure failures, depending on the relationship of $\frac{L}{\sqrt{DT}}$, which used the corrosion defect length (L), pipeline thickness (t) and the pipeline diameter (D). In addition, two conditions are considered in real scale testing. First, limitation of the maximum hoop stress by the material´s yield strength. Second, small profiles of corrosion defect are shown in a parabolic-shape and the corrosion defect length is shown in rectangular-shape [23,38]. In addition, B31 G leads to conservative values, since it used the material yield stress to determine the pressure failure. It is also mentioned that in the B31 G method, the average difference was 27-49%. Filho *et al*. [12] reported an average difference of 25-40% when short corrosion defects in pipelines were evaluated using the B31G method.

The RSTRENG method obtained an average difference of 28-38%. Bedairi [16] reported average differences of 35-37% when they compared this method against the failure pressure predictions for rectangular corrosion defects in API 5L X52 pipelines. The RSTRENG method is based on evidence of experimental failure pressures and simulations by FEM and uses a less conservative bulging factor (M). It is important to emphasize that RSTRENG is limited to low stress concentration. The maximum corrosion defect depth and the external length of corroded area [23] are also considered. In the RSTRENG and B31G methods, the short longitudinal corrosion defects are simplified as parabolic curves. On the other hand, long corrosion defects are simplified as rectangular defects [39]. Another feature of those methods is that the smaller parts are not considered.

Choi *et al*. [14] suggested equations for ideal pits in semi-elliptical defects instead of rectangular and semi-spherical defect. This procedure produces conservative results for larger and deeper corrosion defects in comparison with other methods [13,26], as it is shown in Figs. 6 and 7.

[5] Bulging factor or Folias factor (M), represents the stress concentration due to the bulging that occurs under internal pressure loading [45]

This procedure is based on elliptical and small rectangular corrosion. The failure pressures obtained by Choi's method for a 600 mm corrosion defect length are the lowest valued respective of all methods employed in this study. One can observe this result in Fig. 6a), b) and c). Therefore, this method is not recommended for larger corrosion defect lengths (L> 600 mm).

In the equations proposed by Cronin *et al*. [15] the geometry factor (*g)*, the failure pressure decreases as the corrosion depth increased (Fig. 7), (since the equations involved the relationship of thickness (*t*)), ligament thickness in the deepest part of the defect (t_{LO}), the use of the parameters (α, n of the Ramberg-Osgood parameters) and the critical stress (σ_{Crit}) were not considered.

The failure pressure values for PCORR and DNV methods were close to FEM predictions. For both methods, the bulging factor (M) is less conservative considering that the DNV method multiplies the ultimate tensile stress (UTS) by 2 to obtain the failure pressure [46]. In addition, the maximum stress (σ_{UTS}) of the material is used to obtain the failure pressures. Another important aspect is that these two methods are based on complex corrosion defects. The DNV method is capable of assessing pipelines containing a single defect, multiple interacting defects and complex shaped defects as well as a single defect under internal pressure [17,39].

Although the majority of the well-established methods were validated using FEM and full-scale experiments, different failure pressure values are still being obtained. It can be assumed that the methods used in this paper to obtain failure pressures employed ideal short corrosion defects. However, when the corrosion defect length is larger (L > 600 mm) and the corrosion defect is deeper (about 50% of the pipeline wall thickness), all methods present a mean error (%) in the range of 37-71%. This is because the methods used equations where the variable corrosion defect depth exerts greater influence on the failure pressure estimation than the corrosion defect length, as mentioned in the literature by F. Caleyo *et al*. [5, 47] and J.C Velázquez *et al*. [48] This is understandable since a pipeline with the deepest corrosion defect is more likely to fail than a pipeline with a large and shallow general corrosion defect. The corrosion defect depth has a greater influence on the pipeline strength while the width and length of a corrosion defect has less influence on the pipeline strength. Based on the aforementioned data, the internal pressure leads to rupture [35]. With these conservative values, it is not necessary to repair or remove the pipeline and it could continue in service in some cases [16]. Another condition to be considered is that the methods use ideal corrosion profiles and do not take into account the exact area of corrosion whereas corrosion typically has an irregular profile [41]. In addition, a pit-shaped defect induces high stress concentration making the failure pressures decrease. Although M is the Folias factor (bulging correction factor) and it indicates the stress concentration for pipelines under internal pressure, it is necessary to take into account defects that cause greater stress such as, pitting and edges. In all methods, the width of the corrosion defect was considered having less of an effect on the strength of corroded pipelines and, therefore, this factor was avoided in all assessment equations [42]. Another aspect that is not considered in the methods is the toughness of the material. There are pipelines that have been in service for more than 30 years and have already aged. Fracture toughness is a steel characteristic that should be incorporated into the failure pressure methods; this can help improve the results. However, this is not easy, because facture toughness is estimated by destructive tests. It is well-known that the methods B31 and RSTRENG were developed using pipe steels with low toughness values. While PCORRC and DNV methods used pipe steels with

higher toughness values [43]. For instance, Owen *et al*. [44] obtained a variation of 14-24.5% between the experimentally measured and predicted failure pressure using ASME B31G and ASME B31G modified (RSTRENG).

With the failure pressure values achieved by FEM, it is assumed that this technique considers the actual behavior of material (true stress-strain curve). In this study, the Finite Element Analysis was conducted by the actual properties of the material with a law strain hardening besides constant values of Zenner-Hollomon taken by other authors [23,24], isotropic hardening and Von Mises yielded criterion [12]. Therefore, it is assumed that the behavior of this technique is closer to the actual failure pressure results with these two types of corrosion defects and therefore is less conservative and more realistic. Bedairi *et al*. [16] obtained a percentage of error from 5 to 12.1% when comparing FEM against experimental failure in an API 5L X52 pipeline with rectangular corrosion defects. On the other hand, Alang *et al*. [39] obtained a range error from 4.9 to 9% when experimental results and FEM for failure pressure values were compared in an API 5L X42 steel pipeline. From an engineering point of view, these differences are acceptable and it can be said that the failure pressure values reached by FEM are correct.

4.4 Mechanical behavior of corrosion defect by FEM

To explain the mechanical behavior of pipelines with a combined corrosion defect, the Von Mises stresses were obtained by FEM. Fig. 9 shows the points of interest in the pipeline for both corrosion defects (general and localized corrosion defects). The points of interest are: edge of corrosion (EC) defect length, bottom of corrosion (BC) defect length, edge of pit (EP), bottom of pit (BP) and bottom of corrosion defect (BCD). Fig. 10 displays the Von Mises stress as a function of the internal pressure variation for a) case 1 with wall thickness of 9.525 mm, b) case 2 with wall thickness of 12.7 mm and c) case 7 with wall thickness of 19.05 mm.

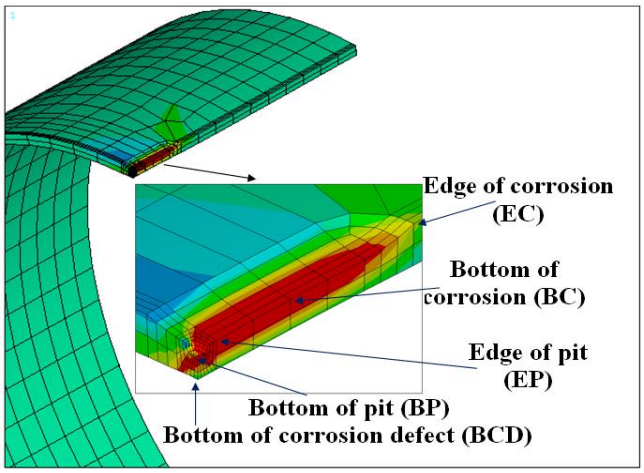

Figure 9. 3D model of a pipeline with a corrosion defect.

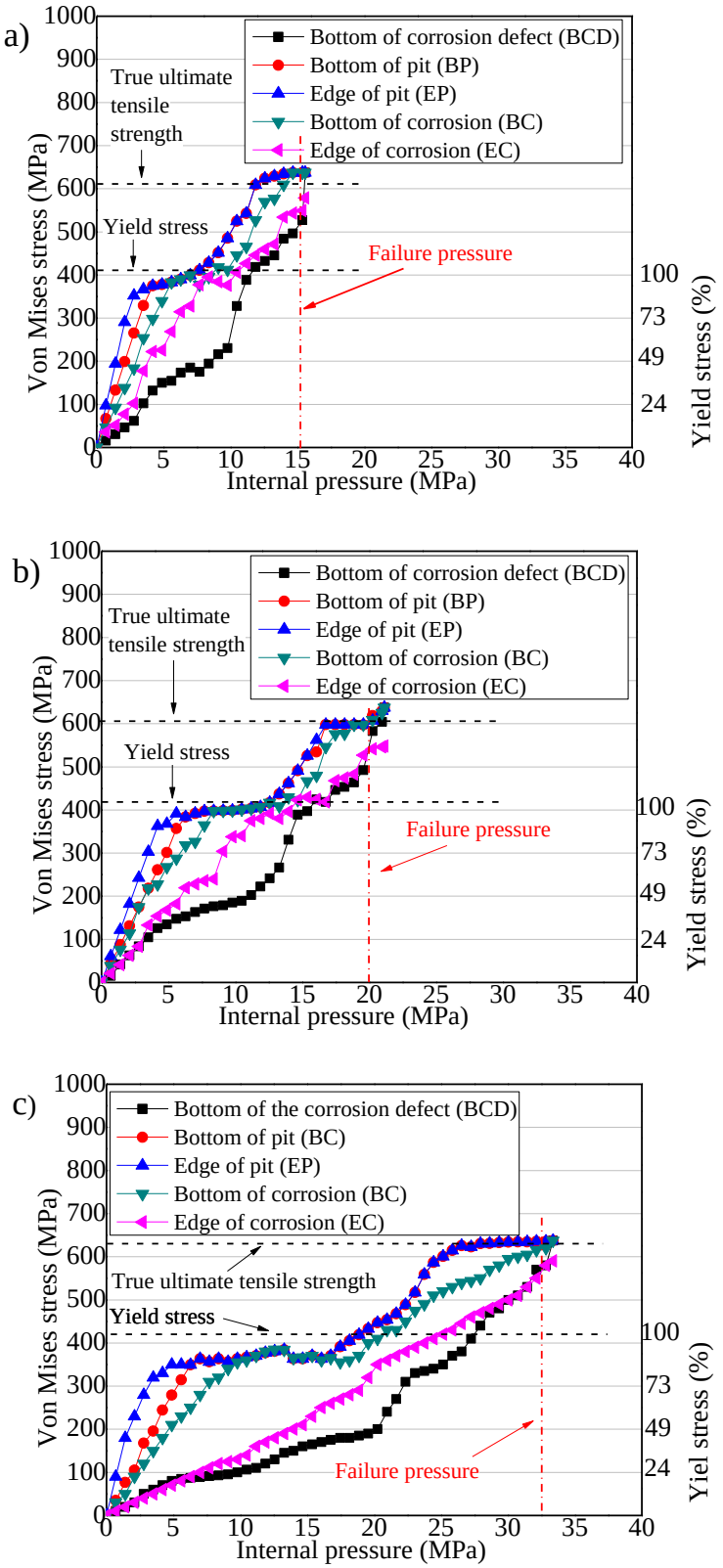

Figure 10. Changes in Von Mises stress states with applied internal pressure load for a) 1, b) 4 and c) 7 conditions.

For all cases (BC, EP and BP) the Von Mises stress varies linearly up to a pressure of 0.3 MPa and corresponds to the 86.5% of the material yield stress strength (σ_{YS}). On the other hand, EC and BCD for all conditions presented low Von Mises stress compared with BC, EP and BC. This is due to the fact that the stresses in EC and BCD acting along the longitudinal direction are higher, resulting in a lower value of Von Mises stress.

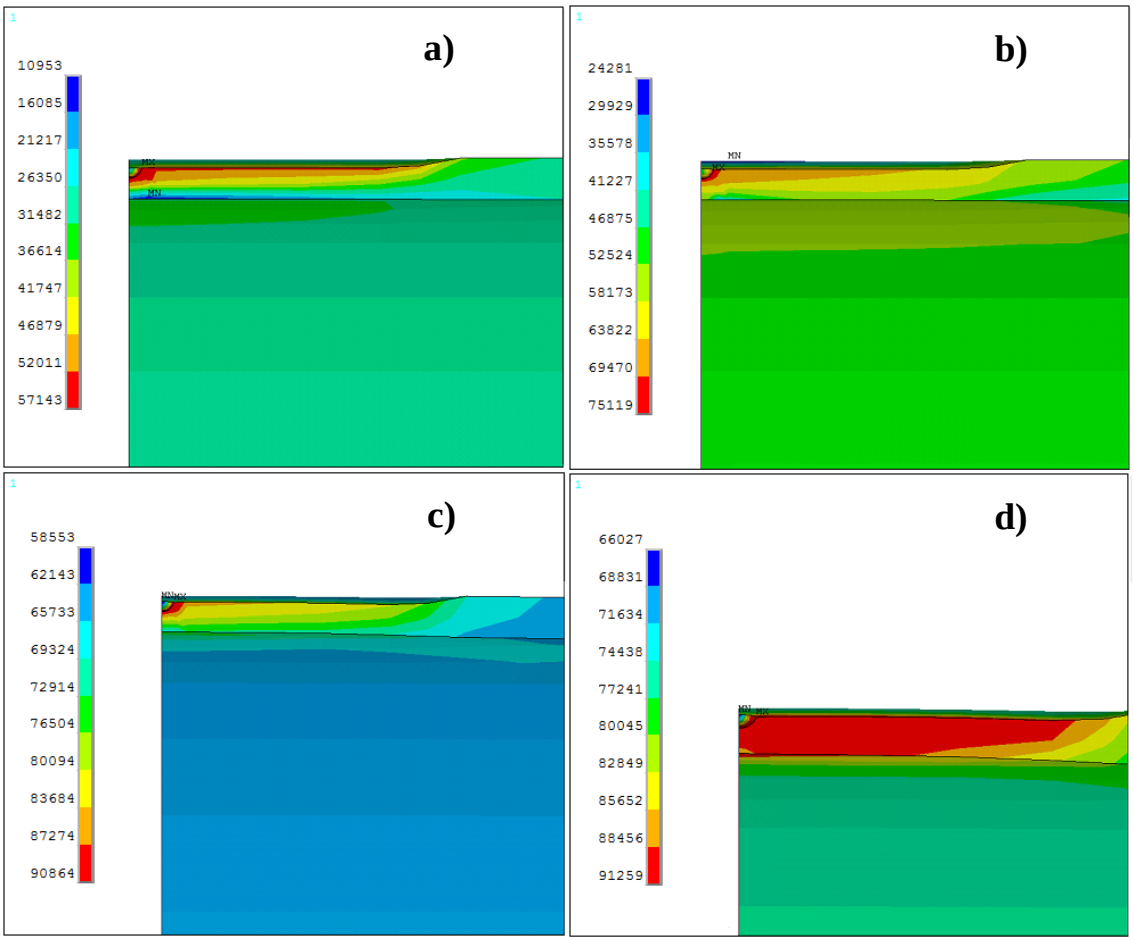

Figure 11. Von Mises stress variation for condition 1 (varying internal pressure)[6]: a) 6.89 MPa, b) 10.34 MPa, c) 13.78 MPa y c) 15.37 MPa.

In practice, the maximum studying pressure for a pipeline is about 70% of the material yield strength [5]. Therefore, local plasticity is not expected in the corrosion defect under normal operating conditions, which present linear elastic behavior. Once the material yield strength has been exceeded, a strain plastic behavior was presented in the ligament and reflected in the loss of linearity in the mechanical behavior of Von Mises stress against the internal pressure. It is therefore safe to state that the pipeline can be operated safely under the σ_{YS}. When the stress exceeds the material yield strength (σ_{YS}), a failure shall be produced in the corrosion defect. BCD and EC points present a different behavior from the other conditions. It could be possible to affirm that for EC and BC points, strain plastic behavior is presented. The strain plastic behavior was reached until the Von Mises stress was

[6] The scale depicted in Fig. 11 and 12 is in pound square inch units (psi)

equal to the yield strength (σ_{YS}) of the material. Therefore, the whole ligament is in the plastic zone, in other words, the entire remaining wall thickness has a plastic behavior. The BC, EP and BP zones exhibit similar behavior.

Since the simulation results for all cases were similar, and for the sake of simplicity, only the analysis for the first condition was described as shown in Table 4. A pipeline with a radius of 304.8 mm, wall thickness of 9.52 mm and a corrosion defect length of 76.2 mm is analyzed. A pressure variation was considered, from 6.9 MPa until it reached the failure pressure values and under the criterion that the failure occurred when the Von Mises stress in the ligament of the corrosion defect was equal to the true tension stress of the material. A pressure variation that reaches plasticity in the ligament is considered, under the criterion that failure occurs when Von Mises stresses in the ligament are equal to the true stress value of the API 5L X52 steel. Fig. 11 a), b), c) and d) display the variation of the Von Mises stress for four different pressures, 6.89 MPa, 10.34 MPa, 13.78 MPa and 15.37 MPa, respectively. At a pressure of P = 15.37 MPa, the ligament has been 100% plasticized. Therefore, the stress at which the pipe fails is reached. The highest stress concentration occurs in the deepest part of the pit (BP) and it extends along the bottom of the generalized corrosion defect (BC), affecting minimal regions of pipeline without strain. This is particularly evident in this case where the stresses are acting more intensely in the longitudinal direction (radial stress σ_1), following the bottom of the corrosion in the longitudinal corrosion (general corrosion).

Fig. 12 shows the Von Mises stress for the pit in which the stress concentration is not symmetrical. Low stress concentration was presented in the circumferential direction (hoop stress, σ_2) and greater concentration was presented in the σ_1. This was attributed to the fact that there was low stress concentration in the outer circumferential side of the pit. The pits usually act as a stress concentration where the greatest stresses were presented in the σ_1 at the bottom of pit (BP), edge of pit (EP), and bottom of corrosion (BC). The greatest stresses and strains are at the bottom of the pit and they extend in the longitudinal direction. Once this area has reached the maximum stresses, the strains are extended, and it is reflected in an increase of the Von Mises stress. Liu *et al.* [35] concluded that the depth corrosion defect depth has the greatest influence in all conditions for failure analysis of the corrosion defects on tubes using FEM. The deeper the corrosion defect, the more severe the stress concentration becomes. The corrosion defects depth appears as the most influential parameter on a pipeline's reliability. Therefore, the failure occurs on the principal plane direction, σ_1, [39]. Chouchaoui *et al*. [28,29] suggested that, in all levels of stress, within the ligament of the pit, the stress is high; therefore, the failure should start within the pit (EP, BP, and BC). This asseveration confirms that the pit fails first. Then, the pipeline failure, with a combined corrosion defect (general corrosion and localized corrosion), is expanded in the bottom of the defect.

It should be interesting for future studies to estimate pipeline failure pressures that include some studies about variations in corrosion defect geometries, pipeline diameters and wall thickness. Besides, it is necessary to include different types of steels and different sizes of corrosion defects [16]. It is confirmed that FEM provides more realistic values of pipeline failure pressure when compared with the experimental results. In this context, it is essential to use FEM to estimate failure pressure predictions in order to understand the mechanical behavior of the pipelines corrosion defects with sophisticated geometries or combined corrosion defects.

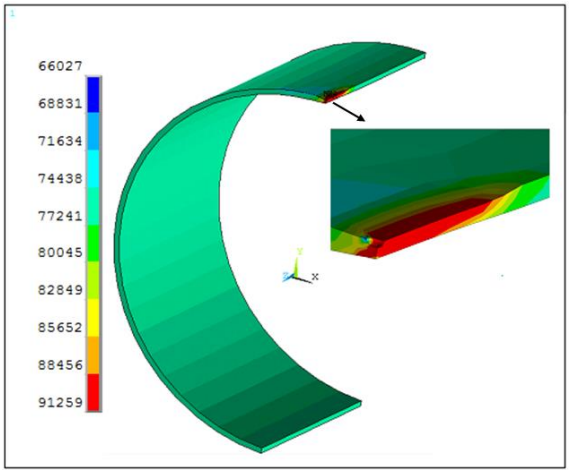

Figure 12. Von Mises stress for condition 1, in pound squared inch (psi).

Obtaining more accurate failure pressure values for pipelines in service, combined with the correct estimation of the corrosion defect depth evolution with modeling techniques for external [49,50] and internal damage [51], is necessary to diminish the risk of pipeline leakage and ruptures. Finally, it is important to notice that probabilistic techniques have also been used in order to determine the reliability level in oil and gas pipelines [52], making it easier to make decisions respecting maintenance investment. A combination of Finite Element Analysis, corrosion defect size evolution and reliability engineering methods can be a challenge for a future study in pipeline integrity.

5. CONCLUSION REMARKS

1. The most conservative methods to estimate the failure pressure in a pipeline with both general corrosion and pitting corrosion in the same corrosion defect are: Shell 92 and Fitnet FFS methods, followed by Choi´s method, B31G, RTRENG-1, Cronin´s method, PCORR and DNV. Failure pressures were also estimated by FEM and, according to the literature, the results obtained are closer to the experimental results. The average differences for Shell-92, Fitnet FFS, Choi´s method, B31G, STRENG-1, Cronin´s method, PCORRC and DNV respecting FEM were 35-47%, 33-46%, 27-72%, 27-49%,26-38%,18-23%,18-37% and 18-40%, respectively.

2. The methods applied in this study based their mathematical expressions on ideal corrosion profiles, such as rectangular defects, parabolic defects, etc. However, they did not take into consideration the real corrosion area, where corrosion typically involves an irregular profile. However, they did not take into account the following considerations: the stress concentration in places with irregular edges, such as pitting, the total width of the corrosion defect and actual pipeline toughness.

3. The well-established methods used in this study are usually applied for short and shallow corrosion defects, getting a better performance. When the corrosion defect is larger (L>600 mm) and deeper than 50% of the pipeline wall thickness, low failure pressures are obtained in the estimation. The failure pressures estimated by the mathematical methods in this study always

underestimated the actual failure pressure. The relative error (RE) obtained in comparison with FEM were always less than 1.

4. According to the results obtained by the Finite Element Method, the mechanical behavior pipeline, with both general corrosion and pitting corrosion in the same corrosion defect, was linear for up to 86.5% of the stress yield of the material. Once the ligament exhibited strain plasticity, the behavior of Von Mises stress deviated from the linearity until reaching the true stress of the material.

5. In a combined corrosion defect (both generalized attack and pitting attack), the stress concentration was not symmetrical. Lower stress in the circumferential direction (hoop stress) and higher stress in the longitudinal direction (axial stress) were discovered. The failure pressure predictions of general corrosion combined with a pit are affected by the length and depth of two corrosion defects. The depth is the principal parameter in the failure pressure predictions.

Appendix A

This appendix shows the mathematical expressions used to estimate the failure pressure in pipelines.

Table A1. Mathematical expressions used to estimate the failure pressure in steel pipelines with corrosion defects.

Failure pressure method	Mathematical expressions
B31G **[6]**	$M = \sqrt{1 + 0.893\frac{L^2}{Dt}}$ $pf = 1.1\frac{2YSt}{D}\left(\frac{1-\frac{2y}{3t}}{1-\frac{2y}{3t}\frac{1}{M}}\right)$ for $\frac{L}{\sqrt{Dt}} \le 4.479$ $pf = 1.1\frac{2YSt}{D}\left(1-\frac{y}{t}\right)$ for $\frac{L}{\sqrt{Dt}} > 4.479$
RSTRENG-1 **[7]**	$M = \sqrt{1 + 0.62756\frac{L^2}{Dt} - 0.003375\left(\frac{L^2}{Dt}\right)^2}$ for $L^2 / Dt \le 50$ $M = 0.032\frac{L^2}{Dt} + 3.3$ for $L^2 / Dt > 50$ $pf = \frac{2(\sigma_{YS} + 68.95MPa)t}{D}\left(\frac{1-0.85\frac{y}{t}}{1-0.85\frac{y}{t}\frac{1}{M}}\right)$
PCORR **[8]**	$pf = \frac{UTS\,t}{D}\left(1-\frac{y}{t}M\right)$

	$M = 1 - \exp\left(-0.157 \frac{L}{\sqrt{D(t-y)/2}} \right)$
DNV-99 **[9]**	$pf = \frac{2UTS\,t}{D-t}\left(\frac{1-\frac{y}{t}}{1-\frac{y}{t}\frac{1}{M}} \right) \quad M = \sqrt{1+0.31\frac{L^2}{Dt}}$
Shell-92 **[10]**	$M = \sqrt{1+0.805\frac{L^2}{Dt}}$ $pf = \frac{1.8UTS\,t}{D}\left(\frac{1-\frac{y}{t}}{1-\frac{y}{t}\frac{1}{M}} \right)$
Fitnet FFS **[11]**	$pf = \frac{2UTS\,t(1/2)^{65/YS}}{D-t}\left(\frac{1-\frac{y}{t}}{1-\frac{y}{t}\frac{1}{M}} \right) \quad M = \sqrt{1+0.8\frac{L^2}{Dt}}$
Choi **[14]**	$for = \frac{l}{\sqrt{rt}} < 6 \quad pf = 0.9\,x\,\frac{2t}{D}\sigma_{UTS}\left[C_2\left(\frac{l}{\sqrt{rt}} \right)^2 + C_1\left(\frac{l}{\sqrt{rt}} \right) + C_0 \right]$ $C_2 = 0.1163\left(\frac{y}{t} \right)^2 - 0.1053\left(\frac{y}{t} \right) + 0.0292$ $C_1 = -0.6913\left(\frac{y}{t} \right)^2 + 0.4548\left(\frac{y}{t} \right) - 0.1447$ $C_0 = 0.06\left(\frac{y}{t} \right)^2 - 0.1053\left(\frac{y}{t} \right) + 1$ $for = \frac{l}{\sqrt{rt}} \geq 6 \quad pf = \frac{2t}{D}\sigma_{UTS}\left[C_1\left(\frac{l}{\sqrt{rt}} \right) + C_0 \right]$ $C_1 = -0.0071\left(\frac{y}{t} \right) - 0.0126$ $C_0 = -0.9847\left(\frac{y}{t} \right) - 1.1101$
Cronin **[15]**	$pf = p_{Long\,Groove} + \left[p_{Plain\,Pipe} - p_{Long\,Groove} \right] x\ g$ $p_{Long\ Groove} = \frac{\sigma_{Crit}}{r\sqrt{\frac{3}{4}}}\, t_{Lo}\, \exp\left(-\sqrt{\frac{3}{4}}\varepsilon_{Crit} \right) \quad \frac{t_{Lo}}{t} \geq 0.2$ $p_{Plain\,Pipe} = 0.90 x p_{2Inst}$

	$p_{2Inst} = \left(\frac{E\sigma_{YS}^{n-1}}{\sqrt{3}\alpha\ n} \right)^{1/n} \frac{2}{\sqrt{3}} \frac{t}{r\left[\exp\left(\frac{1}{2n} \right) \right]^2}$

ACKNOWLEDGEMENT

The authors thank ESIQIE-IPN, Instituto Mexicano del Petróleo (IMP) and CONACYT for the facilities to perform this study. J.C. Velázquez is grateful to Gerencia de Ingeniería y Costos in Pemex for the information provided. The authors would like to acknowledge and express their gratitude to CONACyT for the SNI distinction as research membership and the monthly stipend received.

References

1. G. Koch, J. Varney, N. Thomson, O. Moghissi, M. Gould, and J. Payer, *International Measure of Prevention, Application, and Economics of Corrosion Technologies Study*, NACE International, Houston TX, USA, (2016).
2. F. Caleyo, L. Alfonso, J. Alcántara**,** and J. M. Hallen, *J. Press. Vess. T.*, 130 (2) (2008) 0217041-0217048.
3. J.C. Velázquez, A. Valor, F. Caleyo, V. Venegas, J.H. Espina-Hernández, J.M. Hallen, and M.R. Lopez, *Oil & Gas J.*, 107 (28) (2009) 56- 62.
4. J.C. Velázquez, A. Valor, F. Caleyo, V. Venegas, J.H. Espina-Hernández, J.M. Hallen, and M.R. Lopez, *Oil & Gas J.*, 107 (27) (2009) 64-73.
5. F. Caleyo, A. Valor, V, Venegas, J. H. Espina-Hernandez, J. C Velázquez, and J.M. Hallen, *Oil & Gas J.*, 110 (10) (2012) 122-130.
6. ASME, ASME-B31G—*Manual for Determining the Remaining Strength of Corroded Pipelines*—A Supplement to ANSI/ASME B31 Code for Pressure Piping, The American Society of Mechanical Engineers, New York, (1991).
7. J.E. Kiefner, and P.H. Vieth, "*A modified criterion for evaluating the remaining strength of corroded pipe*". Final report on Project PR 3-805, Battelle Memorial Institute, Columbus, (1989).
8. N. Leis, and D.R. Stephens, "An alternative approach to assess the integrity of corroded line pipe". Part I current status and II alternative criterion. Proceeding of the Seventh International Offshore and Polar Engineering Conference, Honolulu, USA, May 25-30, (1997).
9. Det Norske Veritas, *Corroded Pipelines*, Recommended Practice RP-F101, Hovik, Norway, (2000).
10. F.J. Klever, G. Stewart and C. Van der Valk, "*New developments in burst strength predictions for locally corrode pipes*" Shell Research B.V., The Netherlands, Publication 1306, March, 1995, Offshore Mechanics and Arctic Engineering (OMAE) Conference, Copenhagen, Denmark, (1995).
11. Q. Qian, M. Niffenegger, and S. Li, *Corros. Sci.*, 53 (2011), 855-61.
12. F.J.E. Adalla, R.D. Machado, R.J. Bertin, and M.D. Valentini, *Comput. Struct.*, 132 (2014), 22-33.
13. B. Medjo, M. Rakin, M. Arsic, Z. Sarkocevic, M. Zrilic, and S. Putic, *Materials Transactions*, 53 (1) (2012), 185-90.
14. J.B. Choi, B.K. Goo, J.C. Kim, Y.J. Kim, and W.S. Kim, *Int J. Pres Ves Pip.*, 80 (2003), 121-28.
15. D.S. Cronin, and R.J. Pick, *Int. J. Pres. Ves. Pip.*, 79 (2002), 279-87.
16. B. Bedairi, D. Cronin, A. Hosseini, and A. Plumtree, *Int. J. Pres. Ves. Pip.*, 96-97 (2012), 90-99.
17. L.Y. Xu, and Y.F. Cheng, *Int. J. Press. Ves. Pip.*, 89 (2012), 75-84.
18. W. Zhou, and G.X. Huang, *Int. J. Pres. Ves. Pip.*, 99-100 (2012) 1-8.
19. B. Ma, J. Shuai, D. Liu, and K. Xu, *Eng. Fail. Anal.*, 32 (2013), 209-19.
20. Y.K. Lee, Y.P. Kim, M.W. Moon, W.H. Bang, K.H. Oh, and W.S. Kim, *Material Science Forum*, 475-479 (2005), 3323-3326.

21. R.D. Machado, F.J.E. Abdalla, and H.Y. Shang, "Structural analysis of corroded pipelines containing complex defects". In: Topping BHV, Papadrakakis M, editors. Proceeding on the Ninth International Conference on Computational Structures Technology. Stirlingshire, United Kingdom: Civil-Comp Press, (2008).
22. T.A. Netto, U.S. Ferraz, and A. Botto, *Int. J. Solids Struct.*, 44 (2007), 7597-7614.
23. H. Adib-Ramezani, J. Jeong, and G. Pluvinage, *Int. J. Pres. Ves. Pip.*, 83 (2006), 420-432.
24. H. Adib, S. Jallouf, C. Schmitt, A. Carmasol, and G. Pluvinage, *Int. J. Pres. Ves. Pip.*, 84 (2007), 123-131.
25. G. Fekete, and L. Varga, *Eng. Fail. Anal.*, 21 (2012), 21-30.
26. M.S.G. Chiodo, and C. Ruggieri C. "Burst pressure predictions of corroded pipelines with long defect", 20th International Congress of Mechanical Engineering, November 15-20, Gramado, RS, Brazil, (2009).
27. D. Mok, R. Pick, A. Glover, and R. Hoff, *Int. J. Pres. Ves. Pip.*, 46 (1991), 195-215.
28. B.A. Chouchaoui, and R.J. Pick, *Int. J. Pres. Ves. Pip.*, 67 (1996), 17-35.
29. B.A. Chouchaoui, and R.J. Pick, *Int. J. Pres. Ves. Pip.*, 57 (1994), 187-200.
30. B. Fu, and M. Kirkwood, "Determination of failure pressure of corroded line pipes using the nonlinear finite element method". Pipeline Technology Conference, Belgium, vol. II; (1995).
31. D.R. Stephens, B. Leis, and D. Rudland, "Influence of mechanical properties and irregular geometry on pipeline corrosion defect behavior", (1997).
32. F. Klever, G. Stewart, A. Clemens, and V. Valk, "New developments in burst strength predictions for locally corroded pipelines", OMAE Vol. V., (1995).
33. C. Popelar, "A plane strain analysis model for corroded pipelines", OMAE Vol. V., (1993).
34. ANSYS Introduction to ANSYS for Release 12.1. (2009).
35. X. Liu, H. Zhang, M. Li, Q. Duan, and Y. Chen, *Int. J. Electrochem. Sci.,* 11(2016) 5180-5196.
36. R.S. Motta, S.M.B. Alfonso, R.B. Willmersdorf, P.R.M. Lyra, and E.Q. De Andrade, *Mecánica Computacional*, XXIX (2010) 7871-7890.
37. I. Dick, and M. Inegiyemiema, *Int. J. Scientific Eng. Res.,* 5 (11) (2014) 194-207.
38. B. Fu, and M.G. Kirkwood, Predicting failure pressure of internally corroded linepipe using the finite element method. OMAE Volume V, Pipeline Technology, ASME, (1995) 175-184.
39. N.A. Alang, N.A. Razark, K.A. Shafie, and A. Sulaiman, Finite Element Analysis on Burst Pressure of Steel Pipes with Corrosion Defects, 13th International Conference on Fracture, (2013).
40. K. J. Yeom, Y. K. Lee, K. Hwan Oh, and W. Sik Kim, *Eng. Fail. Anal.,* 57 (2015) 553-561.
41. A. Cosham, P. Hopkins, and K.A. Macdonald, *Eng. Fail. Anal.*, 14 (2007) 1245-1265.
42. C. K. Oh, Y.J. Kim, J. H. Baek, Y. P. Kim, and W.S. Kim, *Int. J. Pres. Ves. Pip.,* 84 (2007) 512-525.
43. K.J. Yeom, Y.K. Lee, K. H. Oh, and W.S. Kim, *Eng. Fail. Anal.*, 57 (2015) 553-561.
44. Owen R, Chauhan V, Pipet D, and Morgan G. Assessment of corrosion damage in pipeline with low toughness. In:14th Biennial joint technical meeting on pipeline research, Berlin; (2003).
45. A. Cosham, and P. Hopkins. The pipeline defect assessment manual. Proceedings of IPC 2002. International Pipeline Conference, 29 September – 3 October, Calgary, Alberta, Canada. IPC02-27067, (2002) 1-1 7
46. Norman E. Dowling, Mechanical behavior of materials, Engineering Methods for Deformation, Fracture and Fatigue. Second Edition Prentice Hall, Boston MA, USA, (1999).
47. F. Caleyo, J.L. Gonzalez, and J.M. Hallen, *Int. J. Pres. Ves. Pip.*, 79 (1) (2002) 77-86.
48. J.C. Velázquez, F. Caleyo, J.M. Hallen, O. Romero-Mercado, and H. Herrera-Hernández, *Int. J. Electrochem. Sci.*, 8 (2013) 11356-11370.
49. J.C. Velázquez, F. Caleyo, A. Valor, and J.M. Hallen, *Corrosion,* 65 (5) (2009) 332-342.
50. J.C. Velázquez, F. Caleyo, A. Valor, and J.M. Hallen, *Corrosion*, 66 (1) (2010) 016001-016001-5.
51. J.C. Velázquez, J.C. Cruz-Ramirez, A. Valor, V. Venegas, F. Caleyo, and J.M. Hallen, *Eng. Fail. Anal.*, 79 (2017) 216-231.
52. F. Caleyo, A. Valor, J.C. Velázquez, and J.M. Hallen, "On the Estimation of the Probability of

Failure of Single Corrosion Defects in Oil and Gas Pipeline", NACE Corrosion Risk Management Conference, May 23-25, Houston TX, paper RISK16-8761, (2016).
53. K.S. Lim, N. Yahaya, N. Md. Noor, S.N.F.M.M. Tahir, J.K. Paik, and M.H. Mohd, *Ships Offshore Sruc.*, 12 (2017) 991-1003.
54. L.J. Cosmes-López, E. Arce, J. Torres, J. Vazquez-Arenas, J.M. Hallen, and R. Cabrera-Sierra, *Corrosion*, 67 (11) (2011) 116001-116010.